| Sl. No. | IIT Ropar<br>List of Recent Publications with Abstract<br>Coverage: November, 2021 |
|---|---|
| 1. | A Riesz-Fejér type inequality for harmonic functions<br>S Das, AS Kaliraj - Journal of Mathematical Analysis and Applications, 2021<br><br>**Abstract**: This article presents a Riesz-Fejér type inequality which compares the integral mean of a complex-valued harmonic function along a circle to the same along a pair of diameters. As a consequence, a result pertaining to real sequences is obtained which generalizes a famous inequality due to Hilbert. Some sharpness results are proved. One particular scope for further research is discussed as well. |
| 2. | A Statistical Features Based Generic Passive Islanding Detection Scheme for IIDGs<br>Y Bansal, R Sodhi - IEEE Transactions on Power Delivery, 2021<br><br>**Abstract**: This paper proposes a new passive Islanding detection approach for the Inverter Interfaced Distributed Generators (IIDGs) operating under different control modes. First, a novel index is formulated using the Root Mean Square (RMS) value of the voltage and the frequency information, acquired at the Point of Common Coupling (PCC) of the target DG. The index is then post-processed by estimating the number of peaks and valleys (Npkv) in a cycle using the sliding window concept, which indicates the occurrence of an event. Finally, the nature of the event, i.e., Islanding or non-Islanding, is decided by exploiting the two statistical features viz., Square of RMS (SRMS) of Npkv and Average Crest Factor (ACFm) of the proposed index. The performance of the proposed method (P-IDM) is demonstrated through comprehensive studies in PSCAD/EMTDC for the single bus system. Also, the real-time validation is performed for the IEEE 34 bus Active Distribution System (ADS) using a Hardware-in-the-Loop (HIL) setup comprising of Real-Time Digital Simulator (RTDS) and dSPACE1104. The simulation and hardware results for different test systems indicate that the proposed scheme, being generic in nature, sustains its efficacy under various interface controls of IIDGs. |
| 3. | A strategic review of recent progress, prospects and challenges of $MoS_2$-based photodetectors<br>R Wadhwa1, AV Agrawal, M Kumar - Journal of Physics D: Applied Physics, 2021<br><br>**Abstract**: Two-dimensional layered materials have emerged prominently in the past decade, largely being investigated fundamentally and practically. Their unique layered structure and atomic-scale thickness make them attractive with exclusive electrical and optical properties compared to their bulk counterparts. Molybdenum disulfide ($MoS_2$) is the most widely studied material in the family of transition metal dichalcogenides. The direct and variable bandgap, high carrier mobility, thermal and chemical stability makes it an attractive choice for next-generation photodetector applications. $MoS_2$ heterojunction-based photodetectors offer ultrafast charge transfer and broadband photoresponse, adding more functionality beyond their individual counterparts. Enormous efforts have been devoted to adopting a new strategy that can improve photodetector performance in terms of responsivity and response time. This review briefly discusses the photo-induced current mechanism and performance parameters along with some important aspects to realize better device performance. Here, we critically review the current status and progress made towards $MoS_2$-based photodetectors, followed by a discussion on open challenges and opportunities in their future application. |
| 4. | ADGD'21: 1st Workshop on Synthetic Multimedia-Audiovisual Deepfake Generation and Detection<br>S Winkler, W Chen, A Dhall, P Korshunov - Proceedings of the 29th ACM International Conference on Multimedia, 2021<br><br>**Abstract**: Deepfakes, i.e.synthetic or "fake" media content generated using deep learning, are a |

| | |
|---|---|
| | double-edged sword. On one hand, they pose new threats and risks in the form of scams, fraud, disinformation, social manipulation, or celebrity porn. On the other hand, deepfakes have just as many meaningful and beneficial applications - they allow us to create and experience things that no longer exist, or that have never existed, enabling numerous exciting applications in entertainment, education, and even privacy.<br>While most work has focused on fake images and video alone, the multi-modal, audiovisual aspect is very important to both convincing generation and accurate detection of fake multimedia content. Therefore, we organize ADGD21: 1st Workshop on Synthetic Multimedia - Audiovisual Deepfake Generation and Detection so as to provide a platform for researchers and engineers to share their ideas and approaches in this field. |
| 5. | An elemental sulfur/$CoS_2$-ionic liquid based anode for high-performance aqueous sodium-ion batteries<br>M Kumar, AK Padhan, D Mandal, TC Nagaiah - Energy Storage Materials, 2021<br><br>**Abstract**: Despite having advantages of safety and dominating consumer and electric vehicle market, the progress of aqueous rechargeable battery research is hindered by low capacity anode materials. A game-changing strategy is to use an environmentally benign aqueous electrolyte with earth abundance Na-ion and sulfur. Sulfur promises to be a next-generation electrode material due to its high theoretical capacity and energy density. But the practical application of elemental sulfur in aqueous electrolyte suffer from sharp capacity decay due to the dissolution of polysulfides. Herein, we report 70 % elemental sulfur along with $CoS_2$ and 1-butyl-3-methylimidazolium o,o-bis(2-ethylhexyl) dithiophosphate (BMIm-DDTP) ionic liquid (IL) as anode (S@$CoS_2$-IL) for aqueous rechargeable sodium-ion/sulfur batteries (ARSSB) in 2 M aq. $Na_2SO_4$ electrolyte.The S@$CoS_2$-IL anode delivers an outstanding capacity of 977 mA h $g^{-1}$ (> 91 % of the theoretical capacity of elemental sulfur *i.e.* 1070 mA h $g^{-1}$), at 0.5 C with a stable cycling performance over 100 cycles with > 98 % of capacity retention at 2 C with 100 % of coulombic efficiency. A negligible loss of S was confirmed by UV–Vis spectroscopy and potentiometric titration and anchoring of polysulfide at S@$CoS_2$-IL anode were evidenced by NMR, ESI-mass, Raman and X-ray photoelectron spectroscopy. The synergy between highly active $CoS_2$ and BMIm-DDTP IL from the dynamic coordination of dithiophosphate with $CoS_2$ provides easy access for polysulfides anchoring and fast reaction kinetics which effectively suppresses the dissolution of discharge polysulfides and $HS^-$. The full cell studies using S@$CoS_2$-IL anode with standard $Na_{0.44}MnO_2$ cathode demonstrate an outstanding capacity of 778 mA h $g^{-1}$ w.r.t the weight of S and 104.98 mA h $g^{-1}$ (of total electrodes weight), which is close to the theoretical capacity of 109 mA h $g^{-1}$ with 100 % coulombic efficiency and 91.8 % capacity retention over 400 cycles at 2 C. The excellent performance of this aqueous battery chemistry shows that S@$CoS_2$-IL anode has great potential towards practical application in ARSSB. |
| 6. | An open source library to parse and analyze online collaborative knowledge-building portals<br>AA Verma, SRS Iyengar, S Setia, N Dubey - Journal of Internet Services and Applications, 2021<br><br>**Abstract**: With the success of collaborative knowledge-building portals, such as Wikipedia, Stack Overflow, Quora, and GitHub, a class of researchers is driven towards understanding the dynamics of knowledge building on these portals. Even though collaborative knowledge building portals are known to be better than expert-driven knowledge repositories, limited research has been performed to understand the knowledge building dynamics in the former. This is mainly due to two reasons; first, unavailability of the standard data representation format, second, lack of proper tools and libraries to analyze the knowledge building dynamics.We describe Knowledge Data Analysis and Processing Platform (KDAP), a programming toolkit that is easy to use and provides high-level operations for analysis of knowledge data. We propose Knowledge Markup Language (Knol-ML), a generic |

| | |
|---|---|
| | representation format for the data of collaborative knowledge building portals. KDAP can process the massive data of crowdsourced portals like Wikipedia and Stack Overflow efficiently. As a part of this toolkit, a data-dump of various collaborative knowledge building portals is published in Knol-ML format. The combination of Knol-ML and the proposed open-source library will help the knowledge building community to perform benchmark analysis.Link of the repository: Verma et al. (2020)Video Tutorial: Verma et al. (2020)Supplementary Material: Verma et al. (2020). |
| 7. | An unknotting invariant for welded knots<br>A Gill, K Kaur. M Prabhakar, A Vesnin - Proceedings of the Indian Academy of Sciences (Mathematical Sciences), 2021<br><br>**Abstract**: We study a local twist move on welded knots that is an analog of the virtualization move on virtual knots. Since this move is an unknotting operation we define an invariant, unknotting twist number, for welded knots. We relate the unknotting twist number with warping degree and welded unknotting number, and establish a lower bound on the twist number using Alexander quandle coloring. We also study the Gordian distance between welded knots by twist move and define the corresponding Gordian complex. |
| 8. | Analytical Modelling of a CMOS Inter Spike Interval Decoder for Resistive Crossbar based Brain Inspired Computing<br>SK Vohra, S Thomas, M Sakare, DM Das - 25th International Symposium on VLSI Design and Test, 2021<br><br>**Abstract**: The enhanced performance of neuromorphic computing over conventional Von Neumann computing results in high accuracy, energy and area efficient operations. The energy efficient neuromorphic systems process the information in the form of spikes. Neural coding schemes is the critical aspect of neuromorphic computing as it defines the relationship between the input sensory information and the spike train. Inter-spike-interval (ISI) encoding shows the advantages of high information density and energy efficiency over rate encoding. This paper shows the analytical modelling of Inter Spike Interval (ISI) decoding scheme. This decoding scheme uses a CMOS implemented sample and hold circuit for ISI to voltage transformation. The circuit is implemented in the Cadence Virtuoso environment using CMOS 180nm technology for analytical verification of the simulation results. Also, to demonstrate the robustness of the decoder circuit, Monte Carlo simulation is done for mismatch and process variation. |
| 9. | Anti Lock Regenerative Braking Scheme for BLDC-Motor Driven Electric Vehicles<br>A Tiwari, AVR Teja - IEEE 30th International Symposium on Industrial Electronics (ISIE), 2021<br><br>**Abstract**: BLDC motors are used in Electric Vehicles(EV) due to their low maintenance requirement, small size, high efficiency, large starting torque and low noise operation. Anti-lock Braking system(ABS) has been an important safety feature in traditional vehicles. While applying brakes, ABS prevents the wheels from getting locked and keeps the steering in driver's control; thereby reducing accidents. This paper proposes a simple method to control BLDC motor for implementing ABS in EV using a combination of Regenerative Braking, short-circuit braking and mechanical braking while requiring no extra ABS sensors. This method will improve the range of EV along with ensuring driver's safety. MATLAB-SIMULINK environment has been used to do the simulations and the results of the same are discussed in this paper. |
| 10. | Bioactive wound dressings for the management of chronic non healing ulcers (CNHU)–A review of clinical and translational studies<br>S Sarkar, AA Poundarik - Materialia, 2021<br><br>**Abstract**: Chronic non healing ulcers (CNHU) can be designated as a silent pandemic affecting a |

| | |
|---|---|
| | large segment of the world population. It is estimated that 6% of the global population are afflicted by chronic wounds. The International Diabetes Federation predicts that a lower limb is amputated every 30 s, globally. Moreover, recently the National Institutes of Health's (NIH) Research Portfolio Online Reporting Tool (RePORT) has enlisted wounds as a distinct disease category. Tremendous global health burden associated with CNHU warrants more holistic and integrated material systems for wound management. Recent advancements in tissue engineering and regenerative medicine have led to the emergence of advanced bioactive dressings capable of re-correcting the course in non-healing wounds. In that regard, the mainstay of this comprehensive review focuses on the vast array of emerging bioactive dressings under clinical evaluation, or in regular clinical use. These include cellular and acellular matrix products such as dermal substitutes, amnion grafts, 3D bioprinted constructs and newer bioactive dressings under trial. This review strives to serve as a reference point for the wound care practitioners with an up-to-date understanding of the prevalent bioactive dressings and disruptive technology platforms with major data based clinical trial findings, their material science and clinical efficacy, for incorporation in the chronic wound management regime. The review also highlights that acellular dermal matrices and amnion based bioactive dressings offer faster wound resolution and cost effectiveness in comparison to the established standard of care.<br><br>**Graphical Abstract**:<br> 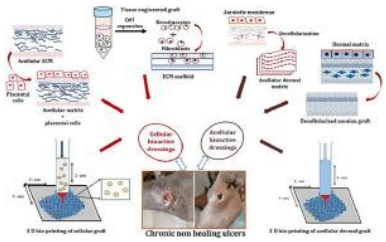 <br> |
| 11. | Comparing the environmental impacts of paracetamol dosage forms using life cycle assessment<br>RK Sharma, G Raju, P Sarkar, H Singh, E Singla - Environment, Development and Sustainability, 2021<br><br>**Abstract**: A medicine can be administered in varied dosage forms which are having different environmental impacts. Two dosage forms of paracetamol (tablet and syrup) have the same function but are prepared and packaged differently, meaning that the environmental impacts arising out of their production will be of different magnitude. This study utilizes the life cycle assessment technique to find and compare the environmental impacts of two dosage forms of the paracetamol. Life cycle assessment software 'GaBi' v 8.0 has been utilized to carry out this study. Midpoint and endpoint impact assessment methods from 'ReCiPe' impact assessment method are used to carry out the life cycle impact assessment. The midpoint impact assessment results show that syrup production has 90% contribution in climate change impact category and more than 50% environment impact in fine particulate matter formation, fossil depletion, freshwater consumption, freshwater eutrophication, freshwater ecotoxicity, ionizing radiation, photochemical ozone formation, stratospheric ozone depletion, and terrestrial ecotoxicity midpoint impact categories. Tablet production has major impacts in 3 midpoint impact categories that are human toxicity, ionizing radiation, and metal depletion. Syrup production has major impacts (more than 70%) in 8 out of the 11 endpoint impact categories considered, while tablet production has a major impact in 3 impact categories that are human toxicity and ionizing radiation endpoint impact categories. Syrup production has a visibly higher impact in more number of midpoint as well as endpoint impact categories considered. The environmental hotspot is, however, dependent on the individual impact categories. The results of the study add to the existing knowledge of environmental sustainability assessment in the pharmaceutical sector and will benefit the environmental managers to better manage the environmental sustainability of |

| | |
|---|---|
| | pharmaceutical products. |
| 12. | Controlled light transport and emission using photonic structures with short-range order<br>SK Saini, RV Nair - Conference on Lasers and Electro-Optics, OSA Technical Digest, 2021<br><br>**Abstract**: We study the resonant frequency gap in the short-range order photonic system. The decay rate measurements are performed for an emitter embedded in these structures to validate the changes in the local density of states. |
| 13. | CORDIC based Orthogonal Signal Generation with In-loop Moving Average Filter for Single Phase PLL Systems<br>S Muddasani, AVR Teja - IECON 2021 – 47th Annual Conference of the IEEE Industrial Electronics Society, 2021<br><br>**Abstract**: In this paper, an Orthogonal Signal Generation (OSG) using CORDIC algorithm is proposed for Phase Locked Loop (PLL) in single-phase systems. The Proposed technique is to overcome the issues of Second Order Generalized Integrator-PLL (SOGI-PLL) in estimating frequency and phase during abnormal conditions (dc offset, harmonics, voltage sag and frequency drift) of the grid. The OSG using CORDIC algorithm along With a Moving Average based band rejection Filter (WMAF) as an in-loop filter is used to attenuate the harmonic frequency components present in the quadrature axis component (V q ) of PLL during abnormal conditions of the grid. To test the effectiveness of the proposed algorithm, the grid voltage input (V g ) with several critical distortions are considered and a comprehensive analysis of the results for the SOGI-PLL, SOGI-PLL-WMAF, and Proposed PLL are presented. These results are simulated using MATLAR/SIMULINK and validated using an experimental setup designed in the laboratory. The frequency estimate and phase are obtained accurately using proposed algorithm under the normal and abnormal conditions of the grid. |
| 14. | Cyclic uniform Lipschitzian mappings and proximal uniform normal structure<br>A Digar, G Kosuru - Annals of Functional Analysis, 2022<br><br>**Abstract**: For $x \in A \cup B$, define $d_n=d(T^n x,T^{n-1}x),n\geq 1$ where A and B are subsets of a metric space and T is a cyclic map on $A\cup B$. In this paper, we introduce a new class of mappings called cyclic uniform Lipschitzian mappings for which $\{d_n\}$ is not necessarily a non-increasing sequence and therein prove the existence of a best proximity pair. We also introduce a notion called proximal uniform normal structure and using the same we prove the existence of a best proximity pair for such mappings. Some open problems in this direction are also discussed. |
| 15. | Design and Development of an Energy-Efficient Oil-Fired Tilting Furnace with an Innovative Recuperator<br>P Singh, H Singh, AK Singh - International Journal of Metalcasting, 2021<br><br>**Abstract**: In this paper, design and development of an energy-efficient oil-fired tilting furnace with an innovative recuperator are reported. During the melting of metals, it is reported that around 50% of the total energy is lost in flue gases. Therefore, there is always a need to improve upon the efficiency of the furnaces. The design of the recuperator is based upon the application of all the three basic modes of heat transfer to preheat the incoming air. Financial and environmental aspects were also evaluated after upgradation with the recuperator. The internal hollow pipe of the proposed recuperator is so designed that at its exterior cylindrical surface, multiple turns of a guide way are welded in a spiral fashion. This increases the heat transfer between the flue gas and ambient air to the burner. The study shows that the efficiency of the oil-fired tilting furnace got enhanced by 50% after implementing the proposed recuperator. Specific fuel consumption without the recuperator was 0.166 kg/kWh, which was reduced to 0.138 kg /kWh with the recuperator. The principle of increasing |

| | |
|---|---|
| | thermal efficiency and limiting fuel consumption was based on heat recovery from the combustion products to preheat the cold incoming fuel mixture. Therefore, this study focuses on the relations between combustion and heat exchanges on a large scale. The exergy evaluation technique was used constructively to estimate the furnace's efficiency since the exergy efficiency is an additional sustainable appraisal in real situations. A channel for flue gases is provided in the developed furnace, which helps to divert hazardous gases away from the working environment. |
| 16. | Design of noble metal-free $CoTiO_3/Zn_{0.5}Cd_{0.5}S$ heterostructure photocatalyst for selective synthesis of furfuraldehyde combined with $H_2$ production<br>S Dhingra, M Sharma, V Krishnan, CM Nagaraja - Journal of Colloid and Interface Science, 2022<br><br>**Abstract**: The development of photocatalytic systems composed of earth-abundant metal-based catalysts for efficient production of clean fuel, H2 as well as value-added chemicals is of significant importance towards sustainable generation of energy resources. Consequently, herein we report rational construction of Z-scheme $CoTiO_3/xZn_{0.5}Cd_{0.5}S$ (x = 5 (S1), 10 (S2), 15 (S3) and 20 wt% (S4)) heterostructures featuring suitable band structure for efficient photocatalytic reduction of protons of water to $H_2$ combined with selective oxidation of furfuryl alcohol (biomass derivative) to a value-added product, furfuraldehyde. Electron microscopy analysis of heterostructure S2 revealed that $Zn_{0.5}Cd_{0.5}S$ nanoparticles are decorated over the surface of CoTiO3 microrods. The photocatalytic studies showed higher catalytic performance by S2, for selective oxidation of furfuryl alcohol to furfuraldehyde with 95% yield coupled with a H2 generation rate of 1929 μmol g−1h−1 which is about 4-fold higher than that of pristine $Zn_{0.5}Cd_{0.5}S$. The enhanced catalytic performance of heterostructure S2 has been ascribed to synergistic interaction aided by the Z-scheme heterojunction formation between $CoTiO_3$ and $Zn_{0.5}Cd_{0.5}S$. Overall, this work demonstrates the application of noble metal-free photocatalyst for simultaneous production of H2 and value-added chemical under mild and environment-friendly conditions.<br><br>**Graphical Abstract**:<br>The development of noble metal-free $CoTiO_3/Zn_{0.5}Cd_{0.5}S$ heterostructures featuring suitable band structure for efficient Z-scheme photocatalytic reduction of protons of water to $H_2$ production combined with selective oxidation of furfuryl alcohol (biomass derivative) to value-added product, furfuraldehyde is demonstrated.<br> 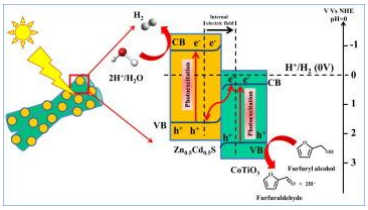 <br> |
| 17. | Development of Cold Sprayed Titanium/Baghdadite Composite Coating for Bio-implant Applications<br>A Kumar, H Singh, R Kant, N Rasool - Journal of Thermal Spray Technology, 2021<br><br>**Abstract**: Titanium/Baghdadite composite coatings have been deposited on SS316L using cold spray technology to explore their potential use as bio-implant coatings. Microstructural and mechanical characterization have been conducted to evaluate the quality of the coatings. The electrochemical corrosion behavior of the developed coatings has been evaluated in a simulated body fluid environment. The results show that baghdadite content influenced the corrosion resistance of coatings; more the baghdadite content, better is the corrosion resistance. In general, the developed coatings were successful in enhancing the corrosion resistance of SS316L. Also, the developed coatings outperformed earlier reported cold sprayed titanium/hydroxyapatite composite coatings. |

| | |
|---|---|
| 18. | Divergence and self-healing of a discrete vortex formed by phase-locked lasers<br>V Dev, V Pal - Journal of the Optical Society of America B, 2021<br><br>**Abstract**: Optical beams carrying orbital angular momentum (optical vortices) are sought for various applications, such as optical communications, optical trapping and manipulation, and material processing. Many of these applications involve the propagation of such beams; therefore, the knowledge of various aspects such as beam size and beam divergence, as well as the effect of beam obstruction, is required. In this paper, we present a numerical study on the generation of high-power discrete vortices by phase locking a 1D ring array of lasers in a degenerate cavity that involves spatial Fourier filtering with a specifically designed amplitude mask. Further, we show that, for a given system size (number of lasers) and fixed distance between the nearest-neighbor lasers, the size of a discrete vortex and its divergence upon propagation do not depend on the orbital angular momentum (topological charge), as opposed to a continuous vortex (Laguerre–Gaussian/Bessel–Gauss beams). We also investigate the self-healing of a discrete vortex by obstructing it at the waist plane ($z$=0) as well as propagation plane ($z$>0), and we show that a discrete vortex possesses good self-healing abilities. The propagation of a truncated discrete vortex has enabled us to identify an unknown topological charge and the rotation dynamics of intensity in a discrete vortex. |
| 19. | Efficient On-chip Communication for Neuromorphic Systems<br>S Kumar, S Das, MM Jamadar, J Kaur - IEEE SmartWorld, Ubiquitous Intelligence & Computing, Advanced & Trusted Computing, Scalable Computing & Communications, Internet of People and Smart City Innovation, 2021<br><br>**Abstract**: Neuromorphic computing is a trending area in computer architecture which deals with the simulation of the brain on hardware. Machine learning problems are very complex to solve by simple computers that work based on Von-Neumann architecture so we need to find architectures that are inspired by the brain and efficient for machine learning, artificial intelligence, and more complex applications. The design has been proposed to implement the traditional software-based Spiking Neural Net-works (SNN) on hardware. However, a major challenge that this SNN based hardware face is the efficient on-chip communications between the neurons. Since SNN has lots of multicast messages to be communicated among the layers, traditional on-chip routing techniques are not sufficient. In this paper, we have proposed a dynamic clustering based on-chip routing mechanism for SNN based hardware. The clustering is based on the dynamic behavior of routers. Compared with the existing clustering-based on-chip routing technique, the proposed technique gives 14% to 38% improvement over average packet latency. |
| 20. | Electrochemical Generation of a Nonstabilized Azomethine Ylide: Access to Substituted N-Heterocycles<br>R Kumar, P Banerjee - The Journal of Organic Chemistry, 2021<br><br>**Abstract**: Azomethine ylides are fascinating 1,3-dipoles for [3 + 2] cycloaddition reactions toward the construction of N-heterocycles. Herein, an efficient and environmentally benign electrochemical approach for the generation of a nonstabilized azomethine ylide has been established under metal-free and external oxidant-free conditions. The resulting 1,3-dipole undergoes a [3 + 2] cycloaddition reaction with olefins. This electrosynthetic methodology indulges a straightforward and facile approach for the construction of substituted pyrrolidines.<br> 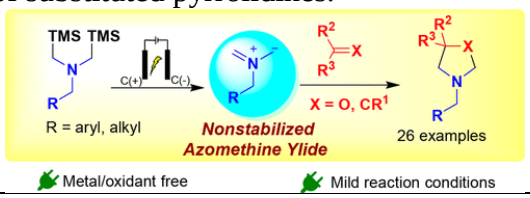 |

| | |
|---|---|
| 21. | Electrohydrodynamics of dielectric droplet collision on different wettability surfaces<br>N Sahoo, D Samanta, P Dhar - Physics of Fluids, 2021<br><br>**Abstract**: In this article, we report the experimental and semi-analytical findings to elucidate the electrohydrodynamics (EHD) of a dielectric liquid droplet impact on superhydrophobic (SH) and hydrophilic surfaces. A wide range of Weber numbers (We) and electro-capillary numbers ($Ca_e$) are covered to explore the various regimes of droplet impact EHD. We show that for a fixed We ~ 60, droplet rebound on a SH surface is suppressed with increase in electric field intensity (increase in $Ca_e$). At high Cae, instead of the usual uniform radial contraction, the droplets retract faster in an orthogonal direction to the electric field and spread along the direction of the electric field, inducing large electrical stresses at the liquid rim facing the electrodes. This prevents the accumulation of sufficient kinetic energy to achieve the droplet rebound phenomena. For certain values of We and Ohnesorge number (Oh), droplets exhibit somersault-like motion during rebound. Subsequently, we propose a semi-analytical model to explain the field induced rebound phenomenon on SH surfaces. Above a critical $Ca_e \sim 4.5$, EHD instability causes a fingering pattern via evolution of a spire at the rim. Further, the spreading EHD on both hydrophilic and SH surfaces is discussed. On both wettability surfaces and for a fixed We, the spreading factor shows an increasing trend with increase in $Ca_e$. We have formulated an analytical model based on energy conservation to predict the maximum spreading diameter. The model predictions hold reasonably good agreement with the experimental observations. Finally, a phase map was developed to explain the post impact droplet dynamics on SH surfaces for a wide range of We and $Ca_e$. |
| 22. | Electromagnetic Field Configurations for Bladeless Wind Turbines<br>V Bhardwaj, AVR Teja - IEEE 30th International Symposium on Industrial Electronics, 2021<br><br>**Abstract**: This paper proposes different electromagnetic field configurations for Bladeless Wind Turbines. Unlike the rotatory wind turbines, bladeless wind turbines depend on vibration to generate electrical power. The existing blade-less wind turbines use permanent magnets in the electromechanical system used for converting vibration into electrical power. The use of permanent magnets not only makes the system costly but also limits the flexibility of changing the field magnitude and direction. In this paper, an electromagnetic field arrangement suitable for bladeless wind turbines is proposed. Various field coil configurations are presented and analysed using ANSYS@Maxwell@. The results are compared and the best possible field coil configuration is proposed. |
| 23. | Engineering $Cu_2ZnSnS_4$ grain boundaries for enhanced photovoltage generation at the $Cu_2ZnSnS_4/TiO_2$ heterojunction: A nanoscale investigation using Kelvin probe force microscopy<br>Nisika, A Ghosh, K Kaur, RS Bobba, Q Qiao, M Kumar - Journal of Applied Physics, 2021<br><br>**Abstract**: Over the past several years, kesterite $Cu_2ZnSnS_4$ (CZTS) absorber has been investigated comprehensively; however, the performance is still hampered by a large open-circuit voltage deficit associated with CZTS bulk defects and interface recombination. To overcome this trend, we report a facile approach to passivate both defect prone areas, i.e., bulk of CZTS and CZTS interface with a $TiO_2$ buffer layer, simultaneously. The existence of oxygen ambient during $TiO_2$ deposition has modulated the electrical properties of CZTS grain boundaries (GBs) not only inside the bulk but also at the surface of CZTS. The passivation of surface GBs is favorable for CZTS/$TiO_2$ heterojunction electronic properties, whereas passivated bulk GBs improve the carrier transport inside the CZTS absorber. To directly probe the photovoltage generation at the CZTS/TiO2 heterojunction, Kelvin probe force microscopy is conducted in surface and junction modes. The acquired photovoltage map exhibits higher values at the GBs, which reveals an increment in downward band bending after |

| | |
|---|---|
| | oxygen diffusion inside the bulk of CZTS. In point of fact, the enhanced diffusion of oxygen accounts for the suppression of carrier recombination and reduction in dark current. Finally, current–voltage and capacitance–voltage measurements performed on the CZTS/$TiO_2$ heterojunction further validate our outcomes. Our findings provide critical insight into the engineering of CZTS GBs to control electronic properties of CZTS and CZTS/$TiO_2$ heterojunctions. |
| 24. | Evaluation of approaches to estimate discharge indices based on mean sediment load for suspended sediment transport in South Indian catchments<br>S Maheshwari, SR Chavan - International Journal of River Basin Management, 2021<br><br>**Abstract**: Discharge indices based on mean sediment load such as fraction-load (f-load) discharge and functional-equivalent discharge represent long-term sediment transfer through river networks. These discharge indices can be used as design flows for the restoration of river channels and in geomorphic and eco-hydrologic studies. In this paper, lognormal distribution-based and Gamma distribution-based Magnitude-Frequency Analysis (MFA) approaches are evaluated to determine reliable estimates of discharge indices for suspended sediment transport in South Indian catchments. The discharge indices are estimated by considering (i) total suspended sediment load and (ii) fine, medium, and coarse suspended sediment loads, separately, as various fractions of suspended sediments have different hydraulic characteristics, transport behaviour, and effect on the ecological system. Results indicate that the lognormal distribution being heavy-tailed tends to assign considerable frequency densities to higher discharges which results in unreliable and magnified estimates of mean sediment load and subsequent discharge indices for most of the catchments. Overall, the Gamma distribution-based MFA approach is found to yield reliable estimates of the f-load discharge and functional-equivalent discharge in comparison to the lognormal distribution-based MFA approach. |
| 25. | Evolutionary dynamics of rock-paper-scissors game in the patchy network with mutations<br>T Verma, AK Gupta - Chaos, Solitons & Fractals, 2021<br><br>**Abstract**: Connectivity is the safety network for biodiversity conservation because connected habitats are more effective for saving the species and ecological functions. The nature of coupling for connectivity also plays an important role in the co-existence of species in cyclic-dominance. The rock-paper-scissors game is one of the paradigmatic mathematical model in evolutionary game theory to understand the mechanism of biodiversity in cyclic-dominance. In this paper, the metapopulation model for rock-paper-scissors with mutations is presented in which the total population is divided into patches and the patches form a network of complete graph. The migration among patches is allowed through simple random walk. The replicator-mutator equations are used with the migration term. When migration is allowed then the population of the patches will synchronized and attain stable state through Hopf bifurcation. Apart form this, two phases are observed when the strategies of one of the species mutate to other two species: co-existence of all the species phase and existence of one kind of species phase. The transition from one phase to another phase is taking place due to transcritical bifurcation. The dynamics of the population of species of rock, paper, scissors is studied in the environment of homogeneous and heterogeneous mutation. Numerical simulations have been performed when mutation is allowed in all the patches (homogeneous mutation) and some of the patches (heterogeneous mutation). It has been observed that when the number of patches is increased in the case of heterogeneous mutation then the population of any of the species will not extinct and all the species will co-exist. |
| 26. | Examining oxidation in β-NiAl and β-NiAl+ Hf alloys by stochastic cellular automata simulations<br>I Roy, PK Ray, G Balasubramanian - npj Materials Degradation, 2021<br><br>**Abstract**: We present results from a stochastic cellular automata (CA) model developed and |

| | |
|---|---|
| | employed for examining the oxidation kinetics of NiAl and NiAl+Hf alloys. The rules of the CA model are grounded in diffusion probabilities and basic principles of alloy oxidation. Using this approach, we can model the oxide scale thickness and morphology, specific mass change and oxidation kinetics as well as an approximate estimate of the stress and strains in the oxide scale. Furthermore, we also incorporate Hf in the grain boundaries and observe the "reactive element effect", where doping with Hf results in a drastic reduction in the oxidation kinetics concomitant with the formation of thin, planar oxide scales. Interestingly, although we find that grain boundaries result in rapid oxidation of the undoped NiAl, they result in a slower-growing oxide and a planar oxide/metal interface when doped with Hf. |
| 27. | Fast Extraction of Per-Unit-Length Parameters of Hybrid Copper-Graphene Interconnects via Generalized Knowledge Based Machine Learning<br>S Kushwaha, A Attar, R Trinchero, F Canavero, R Sharma, S Roy - 30th Conference on Electrical Performance of Electronic Packaging and Systems, 2021<br><br>**Abstract**: In this paper, a knowledge-based machine learning technique has been presented for estimating the per-unit-length parameters of hybrid copper-graphene interconnect networks. The salient feature of the proposed technique is its ability to be trained using significantly smaller amounts of full-wave electromagnetic (EM) solver data compared to conventional machine learning regression techniques, such as artificial neural networks (ANNs) and support vector machines (SVMs). |
| 28. | Four quadrant operation of SRM drive based on Modulated Torque Sharing Function<br>AK Rana, S Singh, AVR Teja - 47th Annual Conference of the IEEE Industrial Electronics Society, 2021<br><br>**Abstract**: This paper presents the four quadrants operation for switched reluctance motor (SRM) drives based on the modulating torque sharing function (TSF). SRM is a nonlinear motor and has torque ripple issues whenever the two phases overlap. The conventional TSF's have predefined function, which are limited to machine specific and have high torque ripple. In this paper, a modulated TSF is proposed, which modulating the torque profile based on the nonlinear inductance and machine currents. In this paper, the torque sharing function is defined in all the quadrant and modulating based on the outgoing current during overlap period. Different results are obtained and analysed in all the quadrants to see the performance of the SRM.The proposed algorithm is verified using Matlab Simulink, and the results are reported. |
| 29. | HFIP-Assisted Single C–F Bond Activation of Trifluoromethyl Ketones using Visible-Light Photoredox Catalysis<br>I Chatterjee, S Ghosh, ZW Qu, S Pradhan, A Ghosh, S Grimme - Angewandte Chemie International, 2021<br><br>**Abstract**: A visible light photoredox catalytic method for the selective cleavage of single strong C–F bond in trifluoromethyl ketones is reported. Single electron reduction of trifluoromethyl ketones generates difluoromethyl radicals which can be engaged in intermolecular C–C bond formation with N -methyl- N -arylmethacrylamides to furnish fluorine-containing oxindole derivatives in good yields. The reaction shows excellent chemoselectivity with good functional group tolerance under mild conditions. 1,1,1,3,3,3-Hexafluoroisopropanol (HFIP) as a solvent plays a critical role for the selective single C–F bond cleavage. High-level DFT calculations are depicted to shed light on the mechanism. |

| | |
|---|---|
| 30. | High Resolution Initial Rotor Position Estimation of SRM Using Peak Current Detection<br>SK Singh, AK Rana, AVR Teja - 47th Annual Conference of the IEEE Industrial Electronics Society, 2021<br><br>**Abstract**: Existing rotor position estimation schemes strongly depend on prior fed data of inductance models which are subject to phenomenal electromagnetic disturbances, mutual inductance interference which inturn requires high gain bandwidth control logic. With these existing methods, an angle error still lies and gets carried along with when the motor is in rotating conditions. This paper discusses about exact rotor position extraction at standstill for reliable starting procedure without any position sensor. Proposed sensorless method tends to inject high frequency signals for short duration in an 8/6 SRM, thereby peak values of currents of all phases is captured for only 0° to 15° and recorded data is curve fitted to train the machine to detect its rotor position to any arbitrary mechanical degree. Authenticity and feasibility of the proposed algorithm is verified on an 8/6 4-phase SRM through MATLAB/Simulink as a testing platform. |
| 31. | Image-Fusion of Ku-band based SCATSAT-1 and MODIS data for Cloud-free Change Detection over Western Himalayas<br>S Singh, RK Tiwari, V Sood, HS Gusain, S Prashar - IEEE Transactions on Geoscience and Remote Sensing, 2021<br><br>**Abstract**: Image-based fusion is a state-of-art process to extract vital information by combining the two or more images acquired from different satellite sensors. Recently launched (26th September 2016) ISRO's (Indian Space Research Organization) Ku-band (13.5 GHz) based Scatterometer Satellite (SCATSAT-1) as an active microwave sensor can offer the day-night, all-weather monitoring services, which are not possible with the optical-based visible and infrared remote sensing satellites. Therefore, the fusion of optical and microwave data offers the cloud-free detection of earth surface transitions and helps in emergency response to natural hazards, security, and defence. The objectives of the proposed framework are (a) nearest-neighbour based fusion (NNF) of ISRO's SCATSAT-1 and NASA's (National Aeronautics and Space Administration) moderate resolution imaging spectroradiometer (MODIS) optical data, (b) generation of thematic maps using artificial neural network (ANN) based classification of the fused data, (c) detection of spatiotemporal variations via post-classification comparison (PCC) based change detection, (d) cross-referencing with well-defined fusion methods, i.e. Gram-Schmidt (GS), Brovey Transformation (BT) and Ehlers, and (e) Impact analysis of clouds on the input dataset and fusion methods. This study has been conducted over the Western Himalayas to estimate the snow cover changes under cloudy conditions with two datasets i.e., winter and monsoon. The experimental outcomes confirm the efficacy of the proposed framework in the effective removal of clouds, generation of classified maps, and change maps. The present study includes an exhaustive list of applicative situations for cloud-free monitoring using freely and daily based SCATSAT-1 and MODIS datasets. |
| 32. | Islanded Mode Microgrid using Stirling based Biogas Generator and Solar PV systems<br>P Kalkal, AVR Teja - 47th Annual Conference of the IEEE Industrial Electronics Society, 2021<br><br>**Abstract**: In this paper, islanded mode microgrid system using biogas and solar PV is discussed for small power applications (upto 250 W) in remote locations. Biogas generation is done using stirling engine coupled with DC generator which directly converts biogas to electrical power. Solar PV system with double sliding integral control based MPPT tracking is connected in parallel with the biogas system. These two sources are connected in parallel to a flyback converter for stepping up the voltage. This is fed to a single phase inverter which is controlled to give constant 220 V, 50 Hz AC to form a hybrid microgrid. The proposed system and the control scheme is modeled in MATLAB/Simulink and tested at different conditions of solar and biogas availability and the results |

| | |
|---|---|
| | are presented. The proposed system could produce 220 V supply with ≈ 1.5% THD. |
| 33. | Matched Filtering with Gaussian Windowed Frequency Modulated Thermal Wave Imaging for Non-destructive Testing and Evaluation of Mild Steel Sample<br>A Rani, R Mulaveesala - IEEE 4th International Conference on Computing, Power and Communication Technologies, 2021<br><br>**Abstract**: InfraRed Thermography (IRT) is a safe, remote, whole field and quantitative Non-Destructive Testing and Evaluation (NDT&E) technique to obtain subsurface information. In this paper, depth resolvability using matched filtering approach has been explored for Frequency Modulated Thermal Wave Imaging (FMTWI) technique. Further, the spectral reshaping has been performed using Gaussian windowing function to study and compare the variations obtained in the thermal response. The present paper explores proposed techniques on a mild steel sample having six Flat Bottom Hole (FBH) defects using finite element modeling and analysis technique. Results shows high defect detection performance of frequency modulated approach by considering correlation coefficient and time delay as a figure of merit. |
| 34. | Mathematical Modelling and Equivalent Circuit Representation of Bladeless Wind Turbines<br>V Bhardwaj, AVR Teja - 47th Annual Conference of the IEEE Industrial Electronics Society, 2021<br><br>**Abstract**: This paper provides a mathematical model for the bladeless wind turbines working on vortex shedding principle. Unlike conventional wind turbines that work with rotary inputs, bladeless turbines require to generate power from vortex induced vibrations. Hence, it is required to have a mathematical model and equivalent circuit representation to help analyze the bladeless wind turbines and estimate different performance metrics. This may also be used in developing efficient control methodologies. A generalized mathematical model with three different equivalent circuit representations for the electro-mechanical system of a bladeless wind turbine is developed in this paper. |
| 35. | Mobility-based Enhancement for Channel Coordination of IEEE 802.11 p on Vehicular Ad-hoc Networks Over V2I<br>S Al-Shaibany, AA Almohammedi, V Shepelev, S Darshi… - International Conference on Intelligent Technology, System and Service for Internet of Everything, 2021<br><br>**Abstract**: Vehicular Ad-Hoc Networks (VANETs) are a sub form of Mobile Ad-Hoc Network that provide communication among vehicles (V2V) and vehicles to infrastructure (V2I). VANETs have been developed to offer reliable and efficient services on the roads. These services include safety applications (collision warning), and non-safety applications (video and voice). The IEEE 802.11p is an extension of the IEEE 802.11 standard to support wireless access into vehicular environments. However, the IEEE 802.11p standard does not perform well for VANETs under high traffic load and mobility. The is owing to the nature of contention-based channel access mechanism in IEEE 802.11p sharing a common radio frequency. The work in this paper presents a new scheme to improve the channel access coordination of 802.11p for V2I communication under high traffic and mobility. This scheme adaptively adjusts the contention window (CW) based on the times (deadlines) that the vehicles are about to exit the RoadSide Unit (RSU) coverage area. Priority service is given to vehicles with shorter deadlines and vice versa. The Network Simulator (NS-2) v.2.35 is used for simulation. According to simulation results, our proposed scheme outperforms the existing scheme in terms of throughput, packet loss ratio and packet delivery. |

| | |
|---|---|
| 36. | Morality-Based Assertion and Homophily on Social Media: A Cultural Comparison Between English and Japanese Languages<br>M Singh, R Kaur, A Matsuo, SRS Iyengar, K Sasahara - Frontiers in Psychology, 2021<br><br>**Abstract**: Moral psychology is a domain that deals with moral identity, appraisals and emotions. Previous work has primarily focused on moral development and the associated role of culture. Knowing that language is an inherent element of a culture, we used the social media platform Twitter to compare moral behaviors of Japanese tweets with English tweets. The five basic moral foundations, i.e., Care, Fairness, Ingroup, Authority, and Purity, along with the associated emotional valence were compared between English and Japanese tweets. The tweets from Japanese users depicted relatively higher Fairness, Ingroup, and Purity, whereas English tweets expressed more positive emotions for all moral dimensions. Considering moral similarities in connecting users on social media, we quantified homophily concerning different moral dimensions using our proposed method. The moral dimensions Care, Authority, and Purity for English and Ingroup, Authority and Purity for Japanese depicted homophily on Twitter. Overall, our study uncovers the underlying cultural differences with respect to moral behavior in English- and Japanese-speaking users. |
| 37. | NEAT Activity Detection using Smartwatch at Low Sampling Frequency<br>A Dewan, VMV Gunturi, V Naik, KK Dutta - IEEE SmartWorld, Ubiquitous Intelligence & Computing, Advanced & Trusted Computing, Scalable Computing & Communications, Internet of People and Smart City Innovation, 2021<br><br>**Abstract**: Our paper aims to build a classification model to discern the typical NEAT (Non-Exercise Activity Thermogenesis) activities done in a home setting. The concept of NEAT is broadly defined as the energy spent in everything which is not sleeping, eating, or a traditional form of physical exercise. We focus on the following NEAT and non-NEAT activities in this paper - cooking, sweeping, mopping, walking, climbing up, climbing down, and non-NEAT activities (e.g., watching television and working on a desk). This aim is to build a classification model which can work with data sampled at a low frequency of 1Hz. However, building such a classifier is non-trivial because the NEAT activities are not easily separable in low-frequency data. The state-of-the-art in the area of human activity recognition either uses multiple physical devices (e.g., accelerometers on arms, waist, and feet) for data collection or use data that is sampled at high frequency (20Hz or above). In contrast, our model performs NEAT activity recognition using data sampled at 1Hz and from a single smartwatch worn on the dominant hand. Thus, making it more energy-efficient and easily usable for widespread use. We evaluate our proposed model using actual data collected on a smartwatch, and we compare it with alternative models. Our results indicate that the proposed model is able to achieve much higher accuracy than the alternative approaches. |
| 38. | Non-Invasive in Vivo Quantification of Directional Dependent Variation in Mechanical Properties for Human Skin<br>P Lakhani, KK Dwivedi, A Parashar, N Kumar - Frontiers in Bioengineering and Biotechnology, 2021<br><br>**Abstract**: Skin is the body's largest organ, and it shows non-linear and anisotropic behavior under the deformation. This behavior of the skin is due to the waviness and preferred orientation (in a particular direction) of collagen fibers. This preferred orientation of collagen fibers results in natural pre-tension and anisotropy of the skin. The knowledge of natural skin pre-tension and anisotropy is essential during incisions and surgery. The available suction-based devices quantify the anisotropy through the displacement field and cannot measure the stress-strain relation in particular directions. Therefore, in the current study, an in vivo full-field measurement suction apparatus was developed to measure the stress and strain of skin in all planar directions through a single experiment. First, this apparatus was |

| | |
|---|---|
| | tested on silicone substrates of known properties, and then it was used to test the skin of 12 human forearms. Further, to check the effect of hand stability on the measurements, the obtained results of the skin were compared with the results of a standard test performed in the same skin using a steady setup. The consistency between these two results confirms that the stability of the hand does not influence the measurements of skin properties. Furthermore, using the developed apparatus, the skin's anisotropy and its relation with the Kraissl's lines orientation was quantified by measuring the toe and linear moduli at an interval of one degree. The minimum and maximum values of the toe and linear moduli were 0.52 ± 0.09 and 0.59 ± 0.11 MPa, and 3.09 ± 0.47 and 5.52 ± 1.13 MPa, respectively. Also, the direction of maximum moduli was found almost similar to Kraissl's lines' orientation. These results confirm the contribution of skin pre-tension on the anisotropy of the skin. The present apparatus mimics the tissue expansion procedure, where observation of the test may be helpful in the selection of size and shape of the expander. |
| 39. | Non-Lorentzian chaos and cosmological holography<br>A Bagchi, S Chakrabortty, D Grumiller, B Radhakrishnan, M Riegler, A Sinha - Physical Review D, 2021<br><br>**Abstract**: We study chaos in non-Lorentzian field theories, specifically Galilean and Carrollian conformal field theories in two dimensions. In a large central charge limit, we find that the Lyapunov exponent saturates the bound on chaos, conjectured originally for relativistic field theories. We recover the same Lyapunov exponent holographically by a shock-wave calculation in three-dimensional flat space cosmologies, providing further evidence for flat space holography. |
| 40. | Opting DC-voltage Droop Control for WF-VSCs in AC-MTDC grids for Effective Frequency and DC-voltage Support<br>AS Kumar, BP Padhy - 47th Annual Conference of the IEEE Industrial Electronics Society, 2021<br><br>**Abstract**: In a decentralized manner, providing Frequency Support (FS) to the AC integrated Multi-terminal DC (AC-MTDC) grids is requisite from most of the Transmission System Operators (TSO's). Extracting this support from the Wind Farms (WFs) through the DC grid is engrossing researchers. In this paper, unlikely, P V 2 is proposed instead of P f droop control for Wind Farm Voltage Source Converters (WFVSCs) for effective FS. This support is achieved while operating the WFs in a derated mode of operation. Besides, this approach also enhances the DC-voltage support to the MTDC grid. In addition, wind variation is also considered to show the impact of this variation on the Frequency and DC-voltage Support (FDS). Further, the proposed approach is validated by considering two area power systems integrated into the five terminal mesh type DC grid with three various schemes simulated in PSCAD/EMTDC software. |
| 41. | Performance Analysis and Fault Modelling of High Resistance Contact in Brushless DC Motor Drive<br>A Gupta, K Jayaraman, RS Reddy - 47th Annual Conference of the IEEE Industrial Electronics Society, 2021<br><br>**Abstract**: High resistance contact (HRC) is a typical stator fault commonly found in motors. This fault is the result of insulation aging, poor artistry, and damaged surfaces due to corrosion. Consequently, unbalance in the stator current can occur and leads to the deteriorated performance of the motor in terms of torque and speed. HRC fault is emulated by inserting an additional resistance in one of the phases of the stator winding. The voltage equations of the three-phase star-connected BLDC motor with resistance imbalance are established in the machine variables. Based on asymmetry in the impedance of the motor, mathematical equations are formulated to evaluate the harmonics responsible for the motor's faulty operation. The performance of the motor is studied by analyzing the variation in stator current, back emf profile, electromagnetic/motor torque, and angular speed. Further, the mathematical expressions of dependent machine variables are developed in terms of fault |

| | |
|---|---|
| | parameters. These expressions demonstrate the deviations of machine variables from their expected values with an increase in fault resistance. Experimental and simulation analysis on 24V 480 W BLDC motor has been done, and the results were obtained to validate the proposed work. |
| 42. | Prediction of De-embedded Eye Height/Width Parameters using Machine Learning in High-Speed Serial Link Characterization<br>M Goyal, M Pandey, S Kumar, R Sharma - IEEE 30th Conference on Electrical Performance of Electronic Packaging and Systems, 2021<br><br>**Abstract**: Post silicon analog validation and characterization refers to a set of activities done on a lab test bench setup to test and debug analog IPs in an SoC (System-on chip). An analog validation engineer typically uses a combination of hardware and software tools to validate an IP. Machine Learning (ML) as a tool has been successfully utilized by engineers in pre-silicon activities like highspeed channel modelling and Eye height/Width prediction. However, very limited research can be found regarding the use of ML algorithms in post silicon analog validation and characterization. Since, post silicon validation's main objective is to find out bugs in system, the accuracy to techniques used in test are of utmost importance. This paper investigates the use of ML in post silicon characterization. This has been done by taking an example use-case: computation of de-embedded signal integrity parameters (Eye Hight and Eye width) from non-de-embedded parameters in the characterization activity of high speed SERDES. It has been shown that by using ML algorithms, one can reduce the SI parameter computation timing with less than 2.1% average error. |
| 43. | Real Life Monitoring of Conveyor Line Speed Using IoT and Raspberry Pi<br>MG Al-Shahethi, A Muneer, EAA Ghaleb, S Darshi, AA Almohammedi - International Conference on Intelligent Technology, System and Service for Internet of Everything, 2021<br><br>**Abstract**: Manual monitoring is time-consuming and frustrates the industry with high costs and delays in the process. This study presented a remote monitoring system for a direct current (DC) motor based on Internet of Things (IoT) for safe and economic data communication in industrial fields. A single sensor monitors the DC motor speed and sends it to the Raspberry Pi microcontroller, which sends it to the cloud database for remote monitoring. The system also presents the manual control methods to adjust the motor speed using a simple potentiometer. Therefore, the proposed system has three functions: measuring, monitoring, and controlling. Measuring is based on an optoisolator sensor and an Arduino Mega microcontroller. Controlling is based on the Potentiometer, Arduino Uno, and a motor drive circuit. Monitoring is based on Raspberry Pi and ThingSpeak platform. Firstly, the speed sensor HC-020K senses the speed Data. Secondly, Arduino Mega extracts the HC-020K sensor's data as a suitable revolution per minute and sends it to Raspberry Pi. Thirdly, Raspberry Pi sends the data to ThingSpeak's Server. Lastly, based on the experiments performed, the system has proved to be very useful and reliable. |
| 44. | Reservoir crowding in a totally asymmetric simple exclusion process with Langmuir kinetics<br>B Pal, AK Gupta - Chaos, Solitons & Fractals, 2021<br><br>**Abstract**: We study a totally asymmetric simple exclusion process equipped with Langmuir kinetics with boundaries connected to a common reservoir. The total number of particles in the system is conserved and controlled by filling factor μ. Additionally, crowding of reservoir is taken into account which regulates the entry and exit of particles from both boundary as well as bulk. In the framework of mean-field approximation, we express the density profiles in terms of Lambert-W functions and obtain phase diagrams in α−β parameter space. Further, we elucidate the variation of phase diagram with respect to filling factor and Langmuir kinetics. In particular, the topology of the phase diagram is found to change in the vicinity of μ=1. Moreover, the interplay between reservoir crowding and Langmuir kinetics develops a novel feature in the form of back-and-forth transition. The theoretical |

| | |
|---|---|
| | phase boundaries and density profiles are validated through extensive Monte Carlo simulations. |
| 45. | Semi-implicit finite-difference methods to study the spin-orbit- and coherently-coupled spinor Bose–Einstein condensates<br>P Banger, P Kaur, S Gautam - International Journal of Modern Physics C, 2021<br><br>**Abstract**: We develop time-splitting finite-difference methods, using an implicit Backward–Euler and a semi-implicit Crank–Nicolson discretization schemes, to study the spin-orbit-coupled (SO-coupled) spinor Bose–Einstein condensates with coherent coupling in quasi-one- and quasi-two-dimensional traps. The split equations involving kinetic energy and spin-orbit-coupling operators are solved using either a time implicit Backward–Euler or a semi-implicit Crank–Nicolson method. We explicitly develop the methods for pseudospin-1/2, spin-1 and spin-2 condensates. The results for ground states obtained with time-splitting Backward–Euler and Crank–Nicolson methods are in excellent agreement with time-splitting Fourier spectral method, which is one of the popular methods to solve the mean-field models for SO-coupled spinor condensates. We confirm the emergence of different phases in SO-coupled pseudospin-1/2, spin-1 and spin-2 condensates with coherent coupling. |
| 46. | Spin-orbit-coupling-driven superfluid states in optical lattices at zero and finite temperatures<br>K Suthar, P Kaur, S Gautam, D Angom - Physical Review A, 2021<br><br>**Abstract**: We investigate the quantum phase transitions of a two-dimensional Bose-Hubbard model in the presence of a Rashba spin-orbit coupling with and without thermal fluctuations. The interplay of single-particle hopping, strength of spin-orbit coupling, and interspin interaction leads to superfluid phases with distinct properties. With interspin interactions weaker than intraspin interactions, the spin-orbit coupling induces two finite-momentum superfluid phases. One of them is a phase-twisted superfluid that exists at low hopping strengths and reduces the domain of insulating phases. At comparatively higher hopping strengths, there is a transition from the phase-twisted to a finite-momentum stripe superfluid. With interspin interactions stronger than the intraspin interactions, the system exhibits a phase-twisted to ferromagnetic phase transition. At finite temperatures, the thermal fluctuations destroy the phase-twisted superfluidity and lead to a wide region of normal-fluid states. These findings can be observed in recent quantum gas experiments with spin-orbit coupling in optical lattices. |
| 47. | Steady-State Dynamics of Exclusion Process with Local Reversible Association of Particles<br>A Jindal, AB Kolomeisky, AK Gupta - Journal of Statistical Physics, 2021<br><br>**Abstract**: Many biological processes are supported by special molecules, called motor proteins or molecular motors, that transport cellular cargoes along linear protein filaments and can reversibly associate to their tracks. Stimulated by these observations, we developed a theoretical model for collective dynamics of biological molecular motors that accounts for local association/dissociation events representing strong coupling of particles. In our approach, the particles interacting only via exclusion move along a lattice in the preferred direction, while the reversible associations are allowed at the specific site far away from the boundaries. Considering the association/dissociation site as a local defect, the inhomogeneous system is approximated as two coupled homogeneous sub-lattices. This allows us to obtain a full description of stationary dynamics in the system. It is found that the number and nature of steady-state phases strongly depend on the values of association and dissociation transition rates. Microscopic arguments to explain these observations as well as biological implications are also discussed. We then compare the dynamical properties of the proposed model with the earlier studied variant considering weakly coupled particles. Theoretical predictions agree well with extensive Monte Carlo computer simulations. |

| | |
|---|---|
| 48. | Study on piezo-electric flapping wing mechanism for bio-inspired micro aerial vehicles<br>NK Shakya, SS Padhee - Journal of Physics: Conference Series, 2021<br><br>**Abstract**: The Micro Aerial Vehicle (MAV) with a flapping wing configuration is much more efficient and capable of generating substantial lift at low flight speeds and has excellent maneuverability. Different motor-driven mechanisms have been developed to mimic this flapping motion, but these mechanisms introduced mechanical complexity and heavy weight to the system. Piezo-electric based mechanisms have been used to solve these problems, but provide very small flapping amplitudes within the size limitation of MAVs. So some kind of amplification mechanism is needed. In this paper, a flexible wing is created by attaching a polymer skin to a pair of carbon fiber reinforced plastic spars. This wing is connected by means of an elastic-element (EE) to a pair of piezoelectric unimorphs (piezofan). The motion from the piezofan to the wing is transferred through this EE. Simulation has been done by applying sinusoidal voltages of varying frequency to this piezofan and observations have been made for the flapping amplitude of the wing for different stiffness of the EE. It is observed that the amplitude of the peak flapping amplitude initially increases, attains a maximum value, then decreases again with an increase in the stiffness of the EE. It is also observed that as the EE stiffness increases, the corresponding peak of the flapping amplitude shifts towards higher frequency. |
| 49. | The activation-free electroless deposition of NiFe over carbon cloth as a self-standing flexible electrode towards overall water splitting<br>A Kafle, M Kumar, D Gupta, TC Nagaiah - Journal of Materials Chemistry A, 2021<br><br>**Abstract**: Herein is described an efficient and straightforward approach to formulate a self-supported flexible electrode, depositing NiFeS and NiFeP over carbon cloth via convenient electroless deposition, thus eradicating traditionally expensive sensitisation and activation procedures. As-prepared NiFeS@OCC and NiFeP@OCC demonstrate good activity for the oxygen evolution reaction (OER) and reach a current density of 10 mA $cm^{-2}$ at low overpotentials of 220 and 270 mV, respectively, demonstrating comparable activity to the state-of-the-art catalyst RuO2. Moreover, both catalysts retain high OER activities even under various deformations. Both catalysts also exhibit appreciable activity when tested for use in the hydrogen evolution reaction (HER). The encouraging bifunctional activity and stability of these simply designed flexible electrodes under full cell conditions for overall water splitting suggest great potential for practical energy conversion applications that require good activity with high flexibility. |
| 50. | The effect of local reversible dissociation of particles in interactive driven diffusive system<br>A Jindal, N Bhatia, AB Kolomeisky, AK Gupta - Physica A: Statistical Mechanics and its Applications, 2021<br><br>**Abstract**: Motor proteins or biological molecular motors belong to a class of active enzymatic molecules that are responsible for transport and force generation in living cells. They typically operate in large teams and individual protein molecules interact with each other while moving along linear cytoskeleton filaments. Moreover, during their transportation the motors can reversibly dissociate from their tracks. Motivated by these observations, we propose a one dimensional totally asymmetric simple exclusion model for interacting particles that are allowed to reversibly dissociate/associate from a particular site far away from the system boundaries. A theoretical analysis of the model is based on cluster mean-field approximation that allows for a comprehensive description of the stationary properties in the system. It is found that the topology and nature of stationary phase diagrams for varying association/dissociation rates strongly depend on the sign and strength of interactions. Extensive Monte Carlo simulations are implemented to test our theoretical predictions. |

| | |
|---|---|
| 51. | The modern role of boron as a'magic element'in biomedical science: Chemistry perspective<br>S Chatterjee, NMM Tripathi, A Bandyopadhyay - Chemical Communications, 2021<br><br>**Abstract**: The boron was misconstrued as a toxic element for animals, which retarded the growth of boron-containing drug discovery in the last century. Nevertheless, modern applications of boronic acid derivatives are entrancing in biomedical applications later than the declaration that boron is a 'probable essential element' for humans by WHO. Additionally, the approval of five boronic acid-containing drugs by the FDA has vastly impacted the use of boron in medicinal chemistry, chemical biology, drug delivery, biomaterial exploration, pharmacological improvements, and nutrition. This review article focuses on the chemistries attributed to boronic acids at physiological pH, enticing chemists to multidisciplinary applications. Perceptive uses of boronic acid in pharma, chemical biology, along with their prospects and challenges, are also part of the deliberation. Understanding these fundamental chemistries and interactions of boronic acid in biological systems will enable solving future challenges in drug discovery and executing space-age applications. |
| 52. | Theoretical Prediction of a Bi-Doped β-Antimonene Monolayer as a Highly Efficient Photocatalyst for Oxygen Reduction and Overall Water Splitting<br>D Singh, R Ahuja - ACS Applied Materials & Interfaces, 2021<br><br>**Abstract**: The photo-/electrocatalysts with high activities for the hydrogen evolution reaction (HER), oxygen evolution reaction (OER), and the oxygen reduction reaction (ORR) are of significance for the advancement of photo-/electrochemical energy systems such as solar energy to resolve the global energy crisis, reversible water electrolyzers, metal–air batteries, and fuel cells. In the present work, we have systematically investigated the photochemical performance of the 2D β-antimonene (β-Sb) monolayer. From density functional theory investigations, β-Sb with single-atom doping possesses a trifunctional photocatalyst with high energetics and thermal stabilities. In particular, it is predicted that the performance of the HER activity of β-Sb will be superior to most of the 2D materials. Specifically, β-Sb with single atom replacement has even superior that the reference catalysts IrO2(110) and Pt(111) with relatively low overpotential values for ORR and OER mechanisms. The superior catalytic performance of β-Sb has been described by its electronic structures, charge transfer mechanism, and suitable valence and conduction band edge positions versus normal hydrogen electrode. Meanwhile, the low overpotential of multifunctional photocatalysts of the Bi@β-Sb monolayer makes them show a remarkable performance in overall water splitting (0.06 V for HER, 0.25 V for OER, and 0.31 V for ORR). In general, the Bi@β-Sb monolayer may be an excellent trifunctional catalyst that exhibits high activity toward all electrode reactions of hydrogen and oxygen.<br> 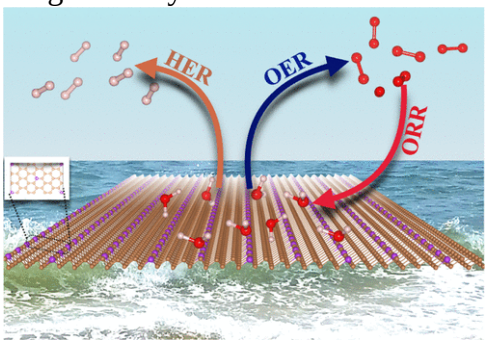 <br> |
| 53. | Thermal design of a humidification-dehumidification desalination cycle consisting of packed-bed humidifier and finned-tube dehumidifier<br>K Garg, SK Das, H Tyagi - International Journal of Heat and Mass Transfer, 2022<br><br>**Abstract**: Humidification-dehumidification (HDH) desalination technology is an ideal technology for |

| | |
|---|---|
| | off-grid and remote locations where fresh water requirement is approximately between 1-100 m3/day. The principal components of the HDH system such as humidifier and dehumidifier have already been utilized in various industrial applications for some time and are readily available in the market. But the actual thermal performance of the HDH system depends on the specific type and size of the components used. In the present study, a detailed heat and mass transfer model has been prepared for a closed-air open-water (CAOW) and water-heated type HDH cycle which uses a counter-flow packed-bed cooling tower for humidification of air and finned-tube heat exchanger for dehumidification purpose. With the help of transport model, the optimum sizes of the humidifier and dehumidifier have been obtained for a desired thermal performance of the cycle, measured in terms of gained output ratio (GOR) and recovery ratio (RR). Additionally, a very basic thermodynamic model for the same HDH cycle is also prepared in order to validate the results of the transport model and results from both the models are found to be in close agreement with each other. Parametric study reveals that for fixed sizes of the humidifier and dehumidifier, there always exists an optimum value of mass flow rate ratio, top brine temperature and feed water temperature at which the GOR of the cycle is maximum. It is also concluded that the thermal performance of the system is greatly influenced by the performance of the dehumidifier as compared to the performance of the humidifier. Finally, the present work will be helpful to design a similar HDH system as per the required GOR and RR.<br><br>**Graphical Abstract**:<br> 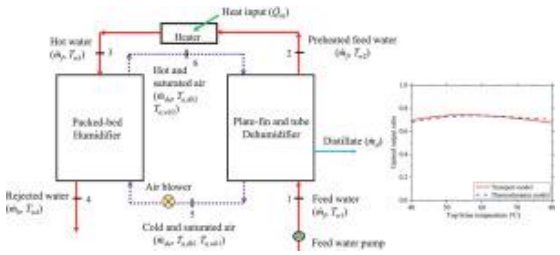 |
| 54. | Tuning the Nanoparticle Interfacial Properties and Stability of the Core–Shell Structure in Zn-Doped $NiMoO_4$@ $AWO_4$<br>P Sharma, MM Sundaram, T Watcharatharapong, S Jungthawan, R Ahuja - ACS Applied Materials & Interfaces, 2021<br><br>**Abstract**: The ability to tune the interfacial region in core–shell nanocomposites with a surface reconstruction as a source for surface energy (de)stabilization is presented. We consider Zn-doped nickel molybdate ($NiMoO_4$) (ZNM) as a core crystal structure and $AWO_4$ (A = Co or Mg) as a shell surface. Based on the density-functional theory method, the interfacial models of Zn-doped $NiMoO_4$@$AWO_4$ (ZNM@AW) core@shell structures are simulated and revealed to undergo surface reconstruction on the (−110) and (−202) surfaces of the AW shells, where the surface degradation of ZNM@MW(−110) is observed. The theoretical simulation is validated against the electrochemical performance of supercapacitor studies. To verify, we synthesize the hierarchical ZNM@AW core@shell semiconductor structured nanocomposites grown on a nickel foam conductive substrate using a facile and green two-step hydrothermal method. The morphology and chemical and electrochemical properties of the hierarchically structured nanocomposites are characterized in detail. The performance of the core@shell is significantly affected by the chosen intrinsic properties of metal oxides and exhibited high performance compared to a single-component system in supercapacitors. The proposed asymmetric device, Zn-doped $NiMoO_4$@$CoWO_4$ (ZNM@CW)‖activated carbon, exhibits a superior pseudo-capacitance, delivering a high areal capacitance of 0.892 F cm–2 at a current density of 2 mA cm–2 and an excellent cycling stability of 96% retention of its initial |

| | |
|---|---|
| | capacitance after 1000 charge–discharge cycles. These fundamental theoretical and experimental insights with the extent of the surface reconstruction sufficiently explain the storage properties of the studied materials.<br> 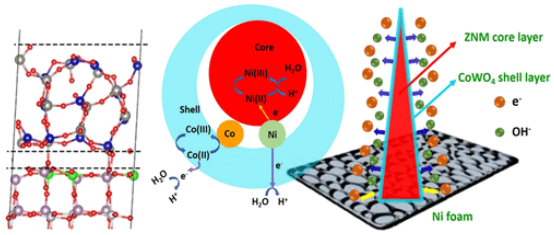 |
| 55. | Tuning the Topographical Parameters of Si Pyramids for a Better Surface Enhanced Raman Response<br>S Midha, J Singh, S Sarkar - Physical Chemistry Chemical Physics, 2021<br><br>**Abstract**: Development of facile routes for the fabrication of surface enhanced Raman substrates (SERS) along with optimal conditions for a high enhancement factor are significant from an application perspective of SERS. Despite steady efforts to establish high SERS signals, cost effectiveness without compromising the enhanced and robust Raman signal remains a major challenge. To address this aspect, herein, we try to tune the topographical aspects of Si pyramidal textures in pursuit of efficient SERS substrates. These pyramidal surfaces are deployed as a pre-template for adopting a SERS substrate using a cost-effective wet chemical etching method. By controlling the etching time, various topographical parameters namely base size, height, pyramidal number density and uniformity of pyramidal textures are modulated. To make all the surfaces SERS active, a Au (50%)–Ag (50%) alloy nanolayer is post-deposited over them. Furthermore, SERS behavior of all the surfaces is investigated by using Rh6G dye as an analyte molecule. In addition to the high density of hot spots in terms of pyramidal number density, base size and uniformity shows a strong correlation in deciding the substantial SERS response. Furthermore, we find a high enhancement factor (~1.42 × 108) for the substrate consisting of dense, small and uniformly sized pyramids. Finite Difference Time Domain (FDTD) simulations done on similar structures corroborate our results. Additionally, universal applicability of the proposed substrate is also verified by detecting methylene blue and methyl parathion analyte molecules. These substrates are much cheaper (~5 USD for 1 × 1 $cm^2$) in comparison with commercially available Klarite SERS substrates (~100 USD for 2 × 2 $mm^2$). We believe this work provides a critical insight into the design of potential SERS substrates using a significantly cost-effective wet chemical etching process. |
| 56. | Ultrasensitive electrochemical biosensors for dopamine and cholesterol: Recent advances, challenges and strategies<br>N Thakur, D Gupta, D Mandal, TC Nagaiah - Chemical Communications, 2021<br><br>**Abstract**: Rapid and accurate determination of dopamine (neurotransmitter) and cholesterol level in bio-fluids is of great significance because they are crucial bioanalytes for several lethal diseases which require early diagnosis. The level of DA in brain is modulated by dopamine active transporter (DAT), which is influenced by the cholesterol levels in the lipid membrane environment. In this context, electrochemical biosensors offer rapid, accurate and exhibit unique features such as low detection limits even with reduced volumes of analyte, affordability, simple handling, portability and versatility, which make them appropriate to deal with presently augmented challenges in current clinical and point-of-care diagnostics for dopamine (DA) and cholesterol determination. The core of this feature article is the the development of ultrasensitive electrochemical biosensors for cholesterol and DA detection for real-time and onsite applications which could detect the targeted analytes at reduced volumes, sub-picomolar concentrations with response times. An ultrasensitive biosensor developed with cost-effective simplified fabrication procedure and displaying high sensitivity, |

| | |
|---|---|
| | selectivity, reliability along with good stability is of supreme worth in the forthcoming era of electrochemical biosensing. Herein, we have put emphasis on recent advanced nanomaterials used for ultrasensitive detection of DA and choleserol and discussed in depth their electrochemical activities towards ultrasensitive reponse. Key points describing future persepective, challenges faced during detection method with their probable solutions is discussed and also surveyed the current market. Further comprehensive studies of various reports open up room for improvement in miniaturization of cholesterol and dopamine biosensors for lab-on-chip devices and overcome current technical limitations to facilitate full utilization by the patients at home. |
| 57. | Vertical Magnetic Field Aided Droplet-impact-magnetohydrodynamics of Ferrofluids<br>N Sahoo, P Dhar, D Samanta - Colloids and Surfaces A: Physicochemical and Engineering Aspects, 2021<br><br>**Abstract**: In this present article, we have investigated the magnetohydrodynamics of ferrofluid droplets impacting on different wettability surfaces, in the presence of a vertical magnetic field. The spreading dynamics was studied for a wide spectrum of magnetic Bond number (Bom), Hartmann number (Ha) and Weber number (We). In absence of any magnetic field, the droplets exhibited secondary droplet pinch-off during rebound. In the presence of magnetic field, the field modulated Rayleigh-Plateau instability delays the droplet pinch off as $Bo_m$ increases. For a fixed We, the rebound of the droplet was suppressed on a superhydrophobic (SH) surface for varying the magnetic field strength (manifested through $Bo_m$). An analytical model based on the principle of conservation of energy was formulated to explain the magnetic field modulated droplet pinch-off. We have also investigated the influence of $Bo_m$ on the temporal spreading dynamics of different Ha ferrofluid droplets impacting on hydrophilic and SH surfaces. With an increase in $Bo_m$, the magneto-visco-capillarity of high Ha droplets inhibits the capillary waves and motion of the contact line after impingement onto hydrophilic surface, compared to low Ha ferrofluid drops. Instead, the droplet rim fragments into secondary droplets during retraction event, leading to the onset of rim instability for low Ha ferrofluid drops with an increase in the magnetic field strength. We have also proposed a theoretical formulation based on energy conservation principle to predict the experimentally measured maximum spreading diameters under influence of magnetic field. The findings may hold significance in ferrofluid based droplet microfluidics systems with magnetic control or actuation.<br><br>**Graphical Abstract**:<br> 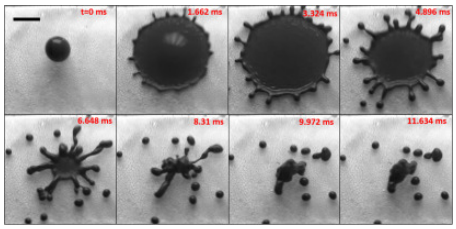 |
| 58. | World War III analysis using signed social networks<br>RR Chowdhury, S Gupta, S Chede - Social Network Analysis and Mining, 2021<br><br>**Abstract**: In the recent period of time with a lot of social platforms emerging, the relationships among various units can be framed with respect to either positive, negative or no relation. These units can be individuals, countries or others that form the basic structural component of a signed network. These signed networks picture a dynamic characteristic of the graph so formed allowing only few combinations of signs that brings the structural balance theorem in picture. Structural balance theory affirms that signed social networks tend to be organized so as to avoid conflictual situations, corresponding to cycles of unstable relations. The aim of structural balance in networks is to find |

| | |
|---|---|
| | proper partitions of nodes that guarantee equilibrium in the system allowing only few combination triangles with signed edges to be permitted in graph. Most of the works in this field of networking have either explained the importance of signed graph or have applied the balance theorem and tried to solve problems. Following the recent time trends with each nation emerging to be superior and competing to be the best, the probable doubt of happening of World War III (WW III) comes into every individuals mind. Nevertheless, our paper aims at answering some of the interesting questions on WW III. In this paper, we have worked with the creation of a signed graph picturing the WW III participating countries as nodes and have predicted the best possible coalition of countries that will be formed during war. Also, we have visually depicted the number of communities that will be formed in this war and the participating countries in each communities. Our paper involves extensive analysis on the various parameters influencing the above predictions and also creation of a new dataset of World War III that contains the pairwise relationship data of countries with various parameters influencing prediction. This paper also validates and analyzes the predicted result. |